J Mater Sci: Mater Electron (2018) 29:993–998
DOI 10.1007/s10854-017-7997-9

Sintering behaviors and microwave dielectric properties of Ti-modified $Ba_3Ti_5Nb_6O_{28}$ ceramics with $35BaO–35ZnO–30B_2O_3$ addition

X. Huang[1,3] · W. J. Wang[1] · J. Lin[1] · D. P. Tang[2] · X. Wu[1] · X. H. Zheng[1]

Received: 9 September 2017 / Accepted: 5 October 2017 / Published online: 11 October 2017

Abstract Effect of $35BaO–35ZnO–30B_2O_3$ (BZB) addition on the sintering behaviors, phase evolution and microwave dielectric properties of Ti-modified $Ba_3Ti_5Nb_6O_{28}$ ($Ba_3Ti_{5.1}Nb_{5.9}O_{27.95}$, BTNO) ceramics had been investigated. BZB addition effectively reduced the sintering temperature of BTNO from 1250 °C to about 900 °C. With increasing BZB addition, the crystal phase of the present ceramics changed from single phase $Ba_3Ti_5Nb_6O_{28}$ to mixing phases of $Ba_3Ti_5Nb_6O_{28}$ and $Ba_3Ti_4Nb_4O_{21}$. And the major phase gradually became from $Ba_3Ti_5Nb_6O_{28}$ to $Ba_3Ti_4Nb_4O_{21}$. Dielectric constant and temperature coefficient increased with the rising of BZB addition. But the Qf value gradually declined from 28000 to about 6000 GHz. The BTNO ceramics with 15% BZB addition exhibited excellent microwave dielectric properties as following: $\varepsilon = 46.3$, $Qf = 5887$ GHz and $\tau_f = 35.5$ ppm/°C, which was potential of candidate materials for LTCC application. And the variation of microwave dielectric properties had been also discussed with the phase and microstructure evolution.

✉ X. H. Zheng
brook76@163.com

[1] Institute of Advanced Ceramics, College of Materials Science and Engineering, Fuzhou University, 2 Xueyuan Road, University Town, Fuzhou 350108, China

[2] College of Zijin Mining, Fuzhou University, 2 Xueyuan Road, University Town, Fuzhou 350108, China

[3] School of Mechanical & Automotive Engineering, Fujian University of Technology, 3 Xueyuan Road, University Town, Fuzhou 350108, China

1 Introduction

With the rapid development of microwave communication system such as mobile system, it requires miniaturization and integration of microwave devices. Low temperature co-fired ceramics (LTCC) multilayer devices have been adopted to meet these requirements [1–5]. It demands that these dielectric ceramics not only have the excellent microwave dielectric properties, but also possess the low sintering temperatures, which is expected to be co-fired with highly conductive internal electrode metals such as Ag and Cu with the low melting point. Although some microwave dielectric ceramics have been found with ultra-low sintering temperature, unfortunately, the sintering temperature of the most investigated microwave dielectric ceramics is too high to limit the LTCC applications [4–10]. For example, the $Ba_{6-3x}(Sm,Nd)_{8+2x}Ti_{18}O_{54}$ ceramics with high-ε and high Qf values, which is widely applied in the mobile system, exhibits high sintering temperature (~ 1350 °C) [9–11]. Therefore, some approaches have been adopted to lower the sintering temperature for meet the requirement of LTCC, which include addition of the glass or oxides with low soft/melting temperature, chemical processing, and using of ultra-fine powder [12–18]. In these approaches, the most economic and effective way is adding glass or oxides with low soft/melting temperature [15–18]. Successful effects have been observed in some dielectric ceramics systems such as TiO_2 [16], $BaO–Ln_2O_3–TiO_2$ [17, 18]. In general, the addition of glass or oxides can reduce the sintering temperature, but it usually deteriorates the microwave dielectric properties. Among these adding glass or oxides with low soft/melting temperature, $BaO–ZnO–B_2O_3$ glass has been widely applied as a low temperature sintering aid. It can not only effectively reduce the sintering temperature, but also remain good microwave dielectric properties. For example,

the BaO–ZnO–B_2O_3 glass not only reduced the sintering temperature of $BaTi_4O_9$ and $Ba_2Ti_9O_{20}$ ceramic from 1350 to about 900 °C, but also made they remain excellent microwave dielectric properties [19, 20]. Thus it is of great interest in industrial application.

Dielectric properties of $Ba_3Ti_5Nb_6O_{28}$ ceramics were investigated by Roberts et al. at 1997 [21]. Later, Sebastian et al. reported $Ba_3Ti_5Nb_6O_{28}$ exhibits microwave dielectric properties of $\varepsilon = 41$, $Qf = 4500$ GHz, $\tau_f = 8$ ppm/°C [22]. And different microwave dielectric properties have also been reported such as $\varepsilon = 37.0$, $Qf = 10{,}600$ GHz, $\tau_f = -12$ ppm/°C [23, 24]. In our previous investigation, it was found that the partial substitution of Nb by Ti significantly improved the microwave dielectric properties of $Ba_3Ti_5Nb_6O_{28}$ ceramics. $Ba_3Ti_{5.1}Nb_{5.9}O_{27.95}$ (BTNO) ceramics displayed excellent microwave dielectric properties of $\varepsilon = 38.3$, $Qf = 28{,}419$ GHz, $\tau_f = -12$ ppm/°C [25]. However, the sintering temperature of pure and Ti-modified $Ba_3Ti_5Nb_6O_{28}$ ceramics is as high as 1250 °C, which is limited the LTCC application. There are few investigations on the low temperature sintering of $Ba_3Ti_5Nb_6O_{28}$ ceramics. Only effects of B_2O_3, CuO and ZnO-B_2O_3 glass on the sintering temperature and microwave dielectric properties of $Ba_3Ti_5Nb_6O_{28}$ ceramics have been investigated [23, 24]. It is not enough for the LTCC application. It is required more work on the low temperature sintering of pure or modified $Ba_3Ti_5Nb_6O_{28}$ ceramics.

Therefore, 35BaO–35ZnO–30B_2O_3 (BZB) oxides have been chosen as a sintering aid to lower the sintering temperature of BTNO ceramics in the present work. And sintering behaviors, crystal phase, microstructure evolution and microwave dielectric properties of BTNO ceramics have been investigated in details.

2 Experimental procedure

Ti-modified $Ba_3Ti_5Nb_6O_{28}$ ceramics of $Ba_3Ti_{5.1}Nb_{5.9}O_{27.95}$ (BTNO) were synthesized by solid state reaction methods. $BaCO_3$ (99.0%), TiO_2 (99.0%) and Nb_2O_5 (99.99%) were weighed and ground for 8 h by ball milling in distilled water. And the milled powder was calcined at 1150 °C for 3 h. 35BaO–35ZnO–30B_2O_3 (BZB) powder were derived from $BaCO_3$ (99.0%), ZnO (99.99%) and H_3BO_3 (99.5%). The calcined powder containing different amount of BZB (0–20 wt%) were reground for 8 h using distilled water. A 5% PVA solution as a binder was added to the dried powder and then the powder were pressed into pellets with 13 mm in diameter and 2–6 mm thick under a pressure of about 100 MPa. The pellets were sintered in the temperature range of 875–1300 °C for 3 h.

Thermogravimetry–differential thermal analysis (TG-DSC, NETZSCH STA 449C) was carried out in air with a heating rate of 10 °C/min from room temperature to 1200 °C. The bulk densities of the sintered samples were determined by the Archimedes method. The crystalline phases were identified by powder X-ray diffraction (XRD, Model D/max-IIIC, Rigaku, Cu K_α, $\lambda = 1.5406 \times 10^{-10}$m). The surface morphology of the samples was detected using a scanning electron microscope (ESEM, Philips XL30 ESEM-TMP). Microwave dielectric properties of sintered samples were measured by $TE_{01\delta}$ mode [26] using a vector network analyzer (Agilent 8362B) and the temperature coefficient (τ_f) of the resonant frequency was measured in the temperature range of 25–85 °C.

3 Results and discussion

Figure 1 shows the TG-DSC plot of BZB power from room temperature to 1200 °C. Below 200 °C, the weight loss is about 11.4%, accompanying two endothermic peaks around 109 and 160 °C, which corresponds to the evaporation of water absorbed and the decomposition of H_3BO_3. From 200 to 800 °C, there are two endothermic peaks at 673 and 787 °C. The peak at 673 °C is corresponding to a large weight loss of 12%. This can be ascribed to the decomposition of $BaCO_3$. And the endothermic peak at 787 °C may be related to the formation of new phase. When temperature is above 800 °C, the weight loss can be ignored. However, a large and broad endothermic peak near 1000 °C is observed in the DSC curve due to the formation of liquid phase.

Figure 2 shows the densities of BTNO ceramics with various amount of BZB addition as a function of sintering temperature. The densities gradually increase with the increase of sintering temperature until they reach the maxima and then saturate. But the density is only about 4.4 g/cm^3 for pure BTNO ceramics sintered at 1200 °C. With the introduction of BZB addition, the densifications of BTNO ceramics

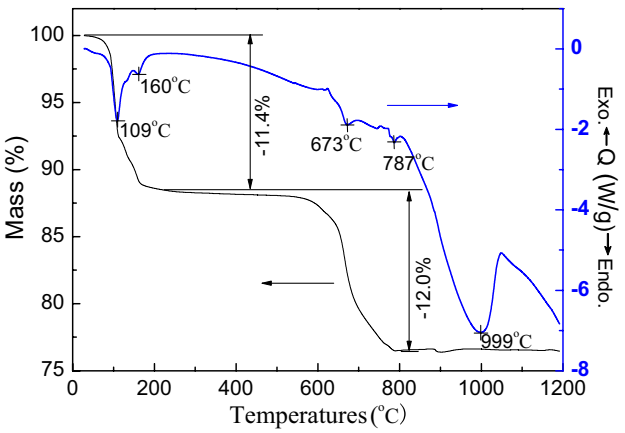

Fig. 1 TG-DSC curves of 35BaO–35ZnO–30B_2O_3 powder

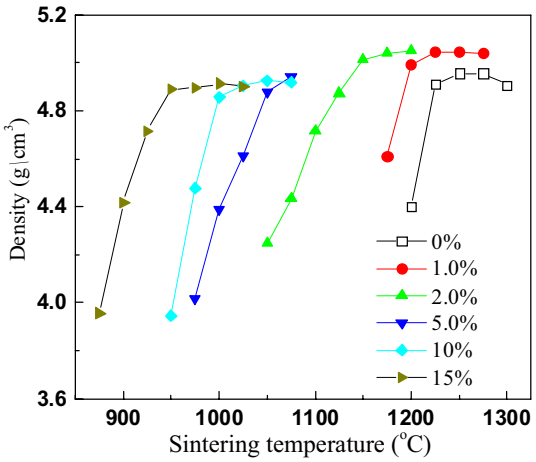

Fig. 2 Density of BTNO ceramics with BZB addition as a function of sintering temperatures

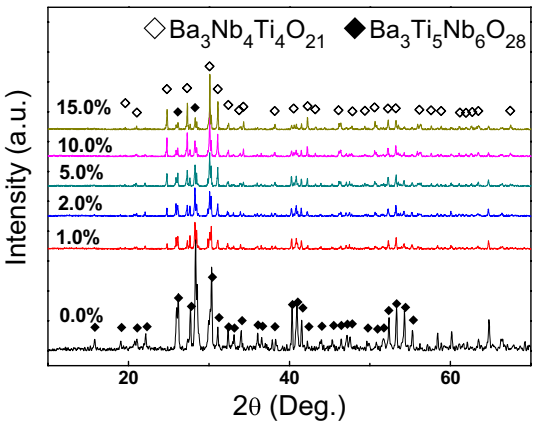

Fig. 3 XRD patterns of BTNO ceramics with BZB addition

are obviously enhanced. When the BZB addition is 1.0%, the densities of samples sintered at 1200–1275 °C are all beyond 5.0 g/cm^3, which is above the largest density of the pure BTNO ceramics. It is clear that the dense temperature of the present ceramics gradually declines with the increase of BZB addition. And the corresponding sintering temperature obviously decreases from 1250 °C for pure BTNO ceramics to about 900 °C for BTNO ceramics with 15% BZB addition. These sintering behaviors of the BTNO ceramics with BZB addition consist well with the DSC analysis of BZB powder. As mentioned above, the liquid phase forms around 1000 °C during the sintering of present ceramics with BZB addition, which effectively enhances the densification of BTNO ceramics.

Figure 3 shows the XRD patterns of BTNO ceramics with BZB addition sintered at optimum temperature. All the diffraction peaks of BTNO ceramics without BZB addition can be indexed according to the $Ba_3Ti_5Nb_6O_{28}$ phase (JCPDS Card No. 37-1477). However, a secondary phase of $Ba_3Ti_4Nb_4O_{21}$ (JCPDS Card No.70-1150) can be detected in the ceramics with a small amount of BZB addition (1.0%). Intensities of diffraction peaks corresponding to $Ba_3Ti_4Nb_4O_{21}$ phase is gradually enhanced with increasing BZB addition, which indicates that the content of $Ba_3Ti_4Nb_4O_{21}$ phase increases. And then the major crystalline phase changes from $Ba_3Ti_5Nb_6O_{28}$ to $Ba_3Ti_4Nb_4O_{21}$ when the amount of BZB addition is up to 5.0%. Because the content of Ba atom in $Ba_3Ti_4Nb_4O_{21}$ is higher than that of $Ba_3Ti_5Nb_6O_{28}$, it may be concluded that the Ba atom in BZB enters the BTNO. This originates from the reaction between BTNO and BZB. And no other crystal phases such as TiO_2, Nb_2O_5 are observed in the present ceramics. So the decomposition of $Ba_3Ti_5Nb_6O_{28}$ ceramics is excluded. And it is noticed that the diffraction peaks of BNTO ceramics become weaker with the introduction of BZB. This suggests that BZB glass phase may be formed during the sintering. Because of the volatility of B^{3+}, the BZB phase may be rich on the surface of samples. As stated above, it can be assumed that BZB addition not only enhances the sinterability, but also reacts with $Ba_3Ti_5Nb_6O_{28}$ to form $Ba_3Ti_4Nb_4O_{21}$.

Figure 4 shows the SEM images of pure BTNO ceramics with BZB sintered at optimum temperature. All the ceramics exhibits little porosity, which is consistent with the high density. Homogeneous microstructure with spherical shaped grains can be observed in the BNTO ceramics. The BTNO samples with a small amount of BZB addition is a dense microstructure with coexistence of the fine grains and large grains, which is related with abnormal growth of grain due to the appearance of liquid phase. For the BNTO ceramics with more BZB addition, the features of the microstructure have large difference from the pure BNTO ceramics. Some densely connected rectangular grains etched by liquid phase can be observed in the ceramics with more BZB addition. This phenomenon agrees with the phase evolution as XRD analysis.

In order to better understand the microstructure and phase evolutions, microstructure of BTNO ceramics with 20% BZB addition have been investigated, which is sintered at different temperature. As shown in Fig. 5, obviously different images are observed for the BTNO sample with 20% BZB addition sintered at 900 and 950 °C. There are many lamellar grains in the sample sintered at 900 °C, but smooth grains for the ceramics sintered at 950 °C. It suggests the more and lower viscous liquid phase exists in the BTNO ceramics sintered at the higher temperature (950 °C). This consists well with the large and broad endothermic peak near 1000 °C of BZB. Consequently, the stronger reaction takes place between BNTO and BZB, which results in denser microstructure and smooth grains. To reveal the phase formation and reaction of BZB, both surface and powder XRD patterns of BTNO sample with 20% BZB addition sintered

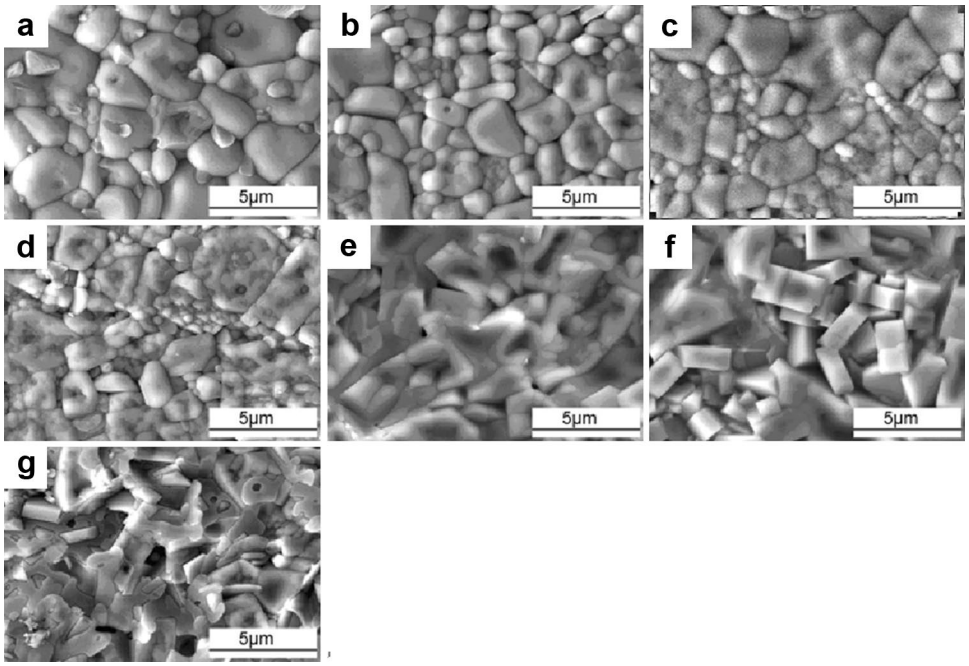

Fig. 4 SEM images of BTNO dense ceramics with BZB addition: **a** 0%; **b** 0.5%; **c** 1.0%; **d** 2.0%; **e** 5.0%; **f** 10.0%; **g** 15.0%

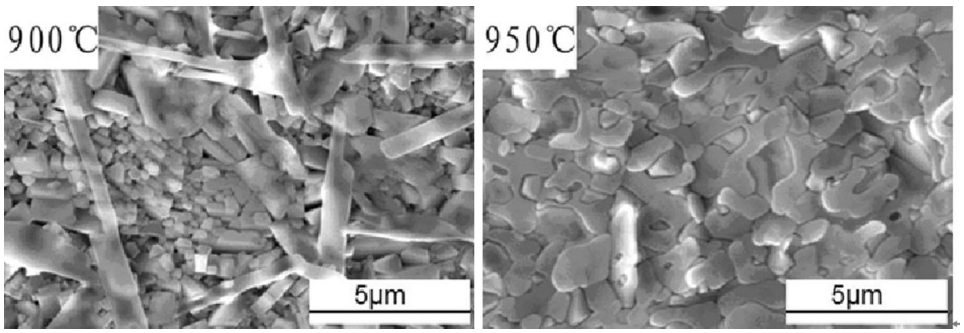

Fig. 5 SEM images of BTNO ceramics with 20.0% BZB addition sintered at different temperature

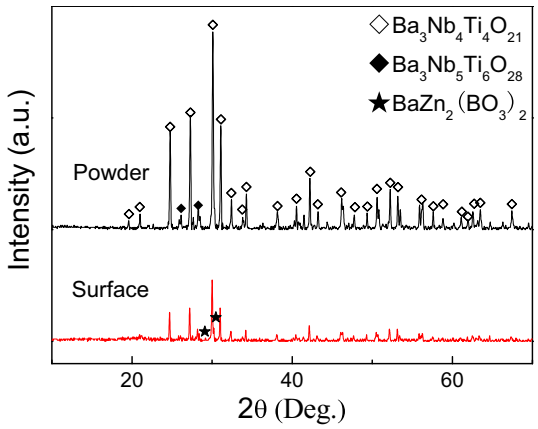

Fig. 6 Powder and surface XRD patterns of BTNO ceramics with 20.0% BZB addition sintered at 900 °C

at 900 °C have also been shown in Fig. 6. XRD patterns of powder are similar to the BNTO ceramics with the more BNB addition such as 15%. Major phase $Ba_3Ti_4Nb_4O_{21}$ and secondary phase $Ba_3Ti_5Nb_6O_{28}$ are observed. But there is obviously difference between the powder and surface XRD patterns. One is the intensities of $Ba_3Ti_4Nb_4O_{21}$ corresponding peaks of in surface XRD are much weaker than those of powder. The other is the diffraction peaks of $BaZn_2(BO_3)_2$ (JCPDS Card No. 81–0830) are detected in surface XRD. It can be inferred that the lamellar grain is $BaZn_2(BO_3)_2$, which is the crystal phase formed around 787.4 °C as shown in DSC curves. As mentioned above, BZB is $35BaO–35ZnO–30B_2O_3$. The content of Ba atom in $BaZn_2(BO_3)_2$ is much lower than that of BZB. So it suggests that some Ba atom enters the $Ba_3Ti_5Nb_6O_{28}$ phase, which results in the formation of $Ba_3Ti_4Nb_4O_{21}$ phase.

Microwave dielectric properties of BTNO ceramics with BZB addition sintered at optimum temperature are shown in Figs. 7 and 8. As shown in Fig. 7, the dielectric

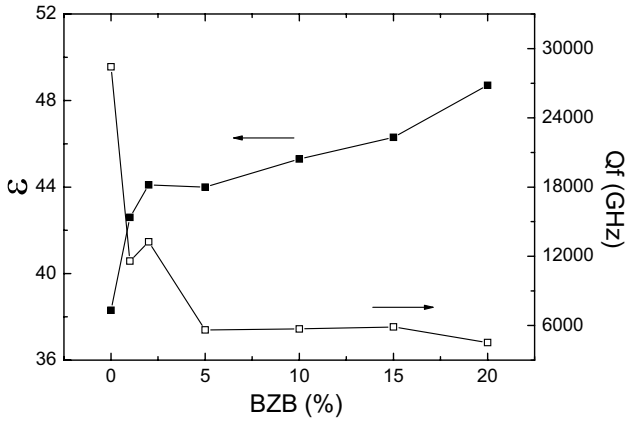

Fig. 7 Dielectric constant and Qf values of BTNO ceramics with BZB addition at microwave frequency

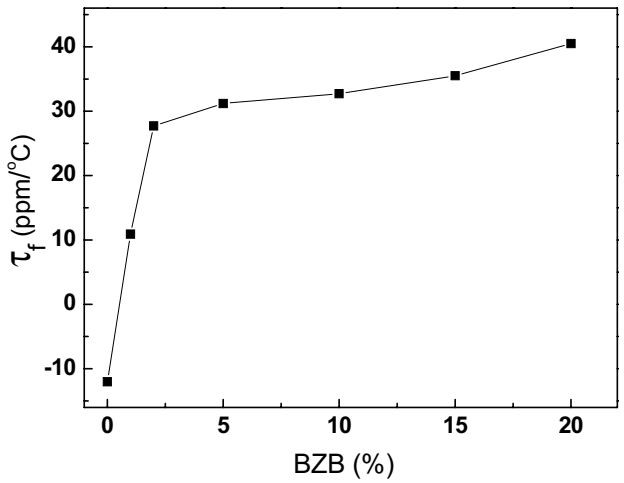

Fig. 8 Temperature coefficient of resonant frequency (τ_f) of BTNO ceramics with BZB addition

constant increases with the increasing of BZB amount. Dielectric constant of Ti-modified $Ba_3Ti_5Nb_6O_{28}$ ceramics and $Ba_3Ti_4Nb_4O_{21}$ ceramics has been reported as 38.3 and 55, respectively [22, 23]. BZB not only enhances the density of BNTO ceramics, but also results in the formation of $Ba_3Ti_4Nb_4O_{21}$ phase with the higher dielectric constant. So the dielectric constant significantly increases from 38.3 for 0% BZB to about 44 for 2% BZB. As mentioned in XRD analysis, with the further increasing BZB addition to 5–20%, the ceramics consists of major phase $Ba_3Ti_4Nb_4O_{21}$, secondary phase $Ba_3Ti_5Nb_6O_{28}$ and glass phase as well as $BaZn_2(BO_3)_2$. And the content of $Ba_3Ti_4Nb_4O_{21}$ phase with the higher dielectric constant gradually increases with the inclining the BZB addition. So the dielectric constant of the present ceramics gradually increases with the rising BZB addition. It is clear found that the variation of dielectric constant is consistent with the variation of phase evolution for the present ceramics.

Compared with dielectric constant, Qf values of the present ceramics have reverse variation with BZB content. At first, Qf value rapidly drops from about 28,000 GHz for BNTO ceramics to about 6000 GHz for the ceramics with 5% BZB, and then has little change.

Generally, Qf value is affected by relative density, secondary phases, impurities, crystal defects, etc. For the present ceramics, it is little variation of relative density. And the sintering temperature has obvious decrease with adding BZB, which maybe inhibit the reduction of Ti^{4+} in BNTO ceramics. So the Qf value of the present ceramics is affected mainly by the secondary phases. The Ti-modified $Ba_3Ti_5Nb_6O_{28}$ ceramics without BZB addition exhibits the highest Qf value of about 28,000 GHz, which is single phase of $Ba_3Ti_5Nb_6O_{28}$ with high Qf value. With the introduction of BZB addition, the glass phase is inevitable appearance. It is well known that network formers contained in the glass phase may profoundly absorb the microwave power due to the resonance type vibration losses, migration losses and deformation losses [27]. Therefore, the Qf value degrades significantly from about 28,000 to near 10,000 GHz when a very amount BZB addition is introduced. When BZB content is not beyond 2%, the ceramics with major phase of $Ba_3Ti_5Nb_6O_{28}$ have the larger Qf value of above 10,000 GHz. However, $Ba_3Ti_4Nb_4O_{21}$ phase and glass phase with low Qf value further increase when BZB addition rises. So the Qf values decrease to about 6000 GHz. But it is higher than most low temperature co-fired ceramics such as $BaO–Ln_2O_3–TiO_2$ based LTCC ceramics [3, 17, 18].

As shown in Fig. 8, it can be found that the τ_f value increases with the increasing of BZB content. The variation of τ_f values can be ascribed to the phase change in the present ceramics. As previous reported [22–25], the τ_f value of $Ba_3Ti_4Nb_4O_{21}$ and Ti-modified $Ba_3Ti_5Nb_6O_{28}$ is about 100 and − 12 ppm/°C, respectively. With the BZB addition increases, $Ba_3Ti_4Nb_4O_{21}$ phase with large positive τ_f value gradually increases, thus the τ_f value of BTNO samples with BZB shifts to positive direction.

4 Conclusions

Sintering behaviors, microstructures and microwave dielectric properties of Ti-modified $Ba_3Ti_5Nb_6O_{28}$ (BTNO) ceramics had been investigated as a function of BZB addition. With increasing BZB addition, the sintering temperature of BTNO ceramics was effectively reduced from 1250 to about 900 °C. $Ba_3Ti_4Nb_4O_{21}$ gradually changed the major phase from the secondary phase, which resulted in the increase of dielectric constant and τ_f. The low-fired BTNO ceramics with 15% BZB addition exhibited excellent

microwave dielectric properties of $\varepsilon = 46.3$, $Qf = 5887$ GHz and $\tau_f = 35.5$ ppm/°C. This indicates that the BTNO ceramics with BZB addition is a promising candidate for LTCC applications.

Acknowledgements This work was supported by the National Natural Science Foundation of China (No. 51602055) and Program for Fujian province development and reform commission (NDRC2013).

References

1. Y.D. Zhang, D. Zhou, J. Am. Ceram. Soc. **99**, 3645–3650 (2016)
2. R. Ratheesh, H. Sreemoolanadhan, S. Suma, M.T. Sebastian, K.A. Jose, P. Mohanan, J. Mater. Sci. **9**, 291–294 (1998)
3. M.T. Sebastian, H. Jantunen, Int. Mater. Rev. **53**, 57–90 (2008)
4. H.H. Xi, D. Zhou, B. He, H.D. Xie, J. Am. Ceram. Soc. **97**, 1375–1378 (2014)
5. X.H. Zhang, Y.M. Ding, J.J. Bian, J. Mater. Sci. **28**, 12755–12760 (2017)
6. G. Zhang, J. Guo, L. He, D. Zhou, H. Wang, J. Koruza, M. Kosec., J. Am. Ceram. Soc. **97**, 241–245 (2014)
7. K. Song, P. Liu, H. Lin, W. Su, J. Jiang, S. Wu, J. Wu, Z. Ying, H. Qin, J. Eur. Am. Ceram. Soc. **36**, 1167–1175 (2016)
8. X. Huang, X. M. Li, D. P. Tang, X. H. Zheng, J. Mater. Sci: Mater. Electron. **26**, 2033–2038 (2015)
9. S.S. Qin, X. Huang, X.H. Zheng, Glass Phys. Chem.**16**, 561–565 (2016)
10. R. Ubic, I.M. Reaney, W.E. Lee, Int. Mater. Rev. **43**, 205–219 (1998)
11. X. Guo, B. Tang, J. Liu, H. Chen, S. Zhang, J. Alloys Compd. **646**, 512–516 (2015)
12. S. Banijamali, T. Ebadzadeh, J. Non-cryst. Solids, **441**, 34–41 (2016)
13. H.J. Lee, K.S. Hong, S.J. Kim, I.T. Kim, Mater. Res. Bull. **32**, 847–855 (1997)
14. R. Chaim, M. Levin, A. Shlayer, C. Estournes, Adv. Appl. Ceram. **107**, 159–169 (2008)
15. F. Amaral, M. A. Valente, L.C. Costa, J. Non-Cryst. Solids, **356**, 822–827 (2010)
16. D.W. Kim, T.G. Kim, K.S. Hong, Mater. Res. Bull. **34**, 771–781 (1999)
17. M.H. Kim, J.B. Lim, S. Nahm, J.H. Paik, H.J. Lee, J. Eur. Ceram. Soc. **27**, 3033–3037 (2007)
18. J. Gao, X. Wang, M. Wang, X. Wang, W. Lu, J. Mater. Sci. **27**, 5954–5959 (2016)
19. M.Z. Jhou, J.H. Jean, J. Am. Ceram. Soc. **89**, 786–791 (2006)
20. L.F. Zhou, H.X. Lin, W. Chen, L. Luo, Jpn. J. Appl. Phys. **47**, 7246–7249 (2008)
21. G.L. Roberts, R.J. Cava, W.F. Peck, J.J. Karjewski, J. Mater. Res. **12**, 526–530 (1997)
22. M.T. Sebastian, J. Mater. Sci. **10**, 475–478 (1999)
23. J.R. Kim, D.W. Kim, S.H. Yoon, K.S. Hong, J. Electro. Ceram. **17**, 439–443 (2006)
24. J.R. Kim, D.W. Kim, I.S. Cho, B.S. Kim, J.S. An, K.S. Hong, J. Eur. Ceram. Soc. **27**, 3075–3079 (2007)
25. J. Lin, Master thesis, Fuzhou university (2010)
26. X.C. Fan, X.M. Chen, IEEE T. Microw. Theory **53**, 3130–3134 (2005)
27. L. Navias, R.L. Gree, J. Am. Ceram. Soc. **29**, 267–276 (1946)